Supramolecular Gelation of Triphenylamine Bis-Urea Macrocycles in Toluene

Rahul Prakash^a, Mohsen Esmaeili^b, Fahidat A. Gbadamosi^a, Monirosadat Sadati^b, Linda S. Shimizu^a,*

^aDepartment of Chemistry and Biochemistry, University of South Carolina, Columbia, South Carolina, 29208, USA. ^bDepartment of Chemical Engineering, University of South Carolina, Columbia, South Carolina, 29208, USA. *Triphenylamine, gels, macrocycle*

ABSTRACT: Herein, we investigate supramolecular gelation behavior of a dendronized triphenylamine bis-urea macrocycle (1) in toluene in the presence and absence of sulfoxide chain stoppers. Macrocycle 1 assembles in the sol phase through intermolecular hydrogen bonding interactions, spontaneously transitioning into a gel state when left undisturbed at room temperature. In toluene, 1 displays a critical gelation concentration of 0.066 wt%, classifying it as a super-gelator. Furthermore, it exhibits a thermoreversible gel-sol phase transition as well as thixotropic behavior. Temperature-dependent ¹H NMR spectroscopy is employed to probe the sol phase assembly of 1 with the size variations at different temperatures assessed by 2D DOSY. Rheological experiments at 10 °C were used to measure gelation response to mechanical stimuli. An amplitude sweep test highlights a linear viscoelastic region. Additionally, the self-healing behavior of gel 1 was verified through a series of strain cycles, where it showed complete recovery. Addition of chain stoppers 10% versus 1 of dimethyl sulfoxide (DMSO) and diphenyl sulfoxide (DPS) lead to weaker gels with smaller differences between the storage and the loss moduli. Rheological analysis revealed slower/partial recovery for the gel containing chain stoppers. Gels assembled from macrocyclic building blocks may retain homogeneous binding cavity and channels offering novel functional properties.

INTRODUCTION

Supramolecular gels represent a distinctive category of supramolecular polymers that combine the solid-like elasticity with the fluid-like micro-viscosity. These gels are colloidal systems characterized by the coexistence of two phases: a liquid-like phase and a solid network, where the solid structure hinders the bulk flow of the liquid component. The solid component frequently consists of fibers; however, it can also take the form of ribbons, platelets, tubular structures, or cylinders. The self-assembly of supramolecular gels is guided by dynamic non-covalent interactions, including hydrogen bonding, π - π interactions, and

van der Waals forces.⁷ As a supramolecular polymer, these gels possess tunable physical characteristics and the ability to respond to stimuli.⁸⁻¹¹ The responsiveness to external stimuli, including temperature, mechanical forces, pH, light, and more, often grants supramolecular gels the ability to undergo a gel-sol phase transition.¹² The dynamic nature of gels makes them promising candidates for a wide range of future applications, including sensing, energy storage, drug delivery, catalysis, gas storage, and waste clean-up.¹³

Gel formation typically begins with the one-dimensional (1D) assembly of monomers through dynamic non-covalent interactions, leading to the propagation of these assemblies

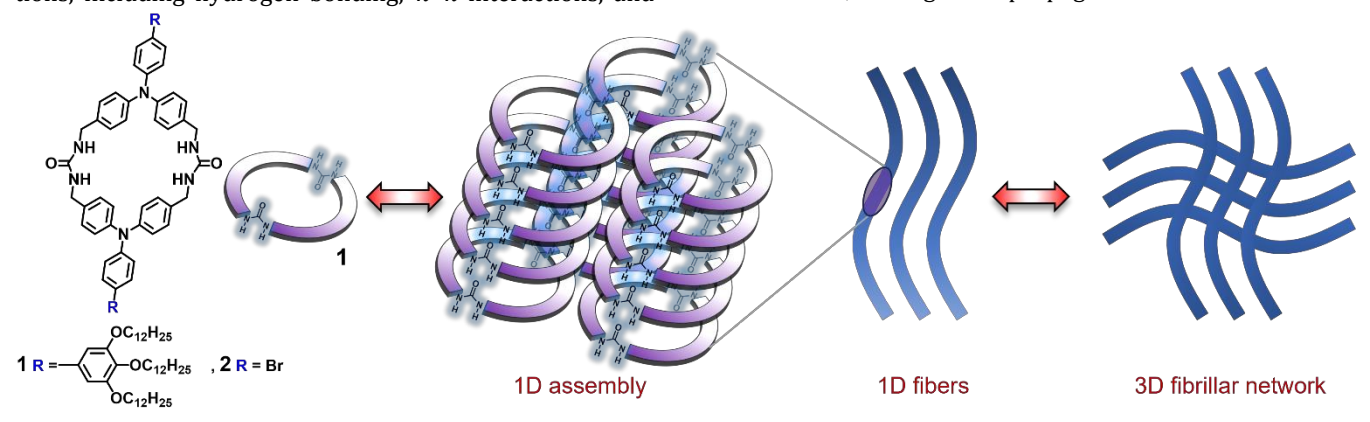


Figure 1 Illustration depicting the dynamic 1D assembly process of macrocycle **1**, leading to the creation of a 3D fibrillar network. In toluene, these 3D fibrous networks culminate in the formation of a gel.

into a fibrillar morphology.^{14,15} These 1D fibrous structures subsequently interweave to form three-dimensional (3D) fibrillar networks, effectively trapping a substantial volume of liquid within them. For this purpose, various macrocycles, such as crown ethers, cyclodextrins, calix[4]arene, calixpyrroles, cucurbit[8]uril, and more, have been reported to exhibit one-dimensional (1D) assembly into fibrous structures.¹⁶⁻²⁰

The Shimizu group has reported bromo-triphenylamine (TPA) bis-urea macrocycles 2 that form columnar crystals with pores that can be employed for single-crystal-to-single-crystal guest exchange, radical generation,21 polymerization of guest molecules,²² and separation of xylene isomers.²³ Recently, the two exterior bromides were replaced with dodecycloxy benzenes affording 1 which retains a similar size internal cavity. Macrocycle 1 assembled cooperatively in H₂O/THF solutions to give one-dimensional (1D) fibers.²⁴ This intriguing fibrous structure of 1 motivated further investigation into its potential for gelation in other solvents. Such gels may retain homogeneous binding channels, which could offer novel functional properties. In this manuscript, we study the formation of a supramolecular gel using monomer 1 in toluene (Figure 1). The assembly in the sol phase is investigated using ¹H NMR, DOSY, and UV spectroscopy. Additionally, rheology characterizes the gel and monitors the impact of chain stoppers on the gelation of 1.

RESULTS AND DISCUSSION

TPA macrocycle **1** was synthesized through a Suzuki coupling reaction between the triazinanone-protected macrocycle **2** and the boronate ester of tridodecycloxy benzene **3** (Scheme S1).²⁴ The synthesis of compound **3** involved three steps, starting with the readily available 5-bromo-1,2,3-trimethoxybenzene. Following the synthesis, the protective group on macrocycle **2** was removed under acidic conditions. The final purification was accomplished by reprecipitation in methylene chloride, yielding the desired TPA macrocycle **1**. The purity of **1** was determined by ¹H NMR, UV-vis, and MALDI-TOF.

Gelation Studies. The preliminary gelation potential of macrocycle 1 was discovered while investigating its solubility in organic solvents. In the case of toluene, at a concentration of 1 mM, macrocycle 1 proved to be insoluble at room temperature. However, upon heating to 60 °C, it dissolved completely, forming a clear solution (Figure 2a). Interestingly, when left at room temperature (approximately 23 °C) for 30 min it transformed into a turbid white gel (determined by tube inversion method). The critical gelation concentration (CGC) of macrocycle **1** at room temperature was determined to be approximately 0.066 wt% (equivalent to 0.057% w/v or 0.3 mM) in toluene. This CGC value of <0.1 wt% categorizes it as a super-gelator.25 The CGC of compound 1 is comparable to that of a crown ether macrocycle (0.06 wt%)²⁵ but significantly lower than that of a giant macrocycle (1.3-1.9 wt%)²⁶ and a diacetylene macrocycle $(0.51 \text{ wt}\%)^{27}$.

The supramolecular gel formed by 1 exhibits a thermoreversible gel-sol transition. When heated to 60 °C, the gel reverts to the sol phase, and this transformation can be reversed by allowing the sol phase to stand undisturbed at room temperature for 30 min. Notably, the gelation property remains stable even after undergoing multiple sol-gel

transitions. Furthermore, this gel also displays self-healing characteristics. When vigorously shaken while in the gel phase, it transforms into a mobile viscous liquid. And when left undisturbed for an hour, it reverts to the gel phase, as confirmed by the inverted tube test.

The structure of gel **1** was analyzed through fluorescence microscopy. A small amount of gel was placed on a glass slide and allowed to air dry, evaporating the solvent. The resulting images captured fibrous structures within the dried gel, with the fibers' width measuring between 500-600 nm in width (Figure 2b).

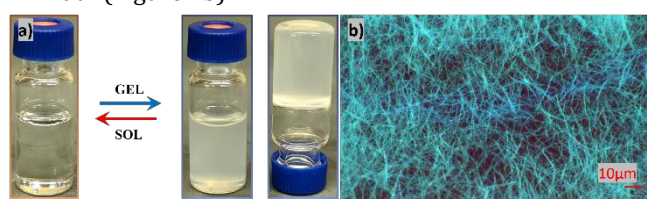


Figure 2 (a)Photographs showing gel formation of **1** in toluene (tube inversion test). Macrocycle **1** was dissolved in toluene by heating at 60 °C (on left). Leaving it at room temperature for 30 min results in gel formation (on right). By heating it again at 60 °C gel can be transitioned to sol phase. (b) Micrograph of the dried gel **1** exhibiting fibrous formations under fluorescence.

Assembly in Sol Phase. Given the TPA chromophore in 1 (λ_{max} = 320 nm, 0.5 mM toluene), assembly in the sol phase was examined by temperature dependent UV-vis spectroscopy. As the sol was cooled from 70 to 14 °C, a decrease in absorbance was observed with a shift to longer wavelength (λ_{max} = 329 nm) and a new shoulder peak at 301 nm (Figure 3a). Extended equilibration at 14 °C also resulted in gel formation. Absorbance at 320 nm vs. temperature (Figure S7a) shows some thermal relaxation until 54 °C after that there is a consistent decrease in absorbance, likely indicative of the gelation process. In comparison, in H₂O/THF the 1-dimensional aggregated fibers of 1 (10 μ M) exhibited a λ_{max} = 370 nm, 22 highlighting the solvent effect.

The sol-gel transition for ${\bf 1}$ was tracked with UV-vis spectroscopy at 22 °C with a concentration of 0.5 mM in toluene. The sol was equilibrated at 22 °C, and absorbance readings were taken every minute, as illustrated in Figure 3b. Over time, the spectra indicated a consistent reduction in absorbance, although the characteristic peaks were preserved. The graph of absorbance at 329 nm against time (Figure S7b) exhibited a sinusoidal decay. This decreasing absorbance over time implies the formation of a gel.

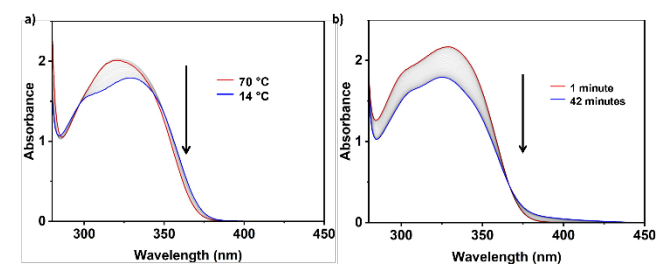


Figure 3 (a) Temperature-dependent UV-vis spectra of **1** in toluene at a concentration of 0.5 mM. Arrow indicates the change in spectra upon cooling from 70 °C to 14 °C. (b) Time-dependent UV-vis spectra of **1** at 22 °C and 0.5 mM. The Arrow indicates change in spectra with time.

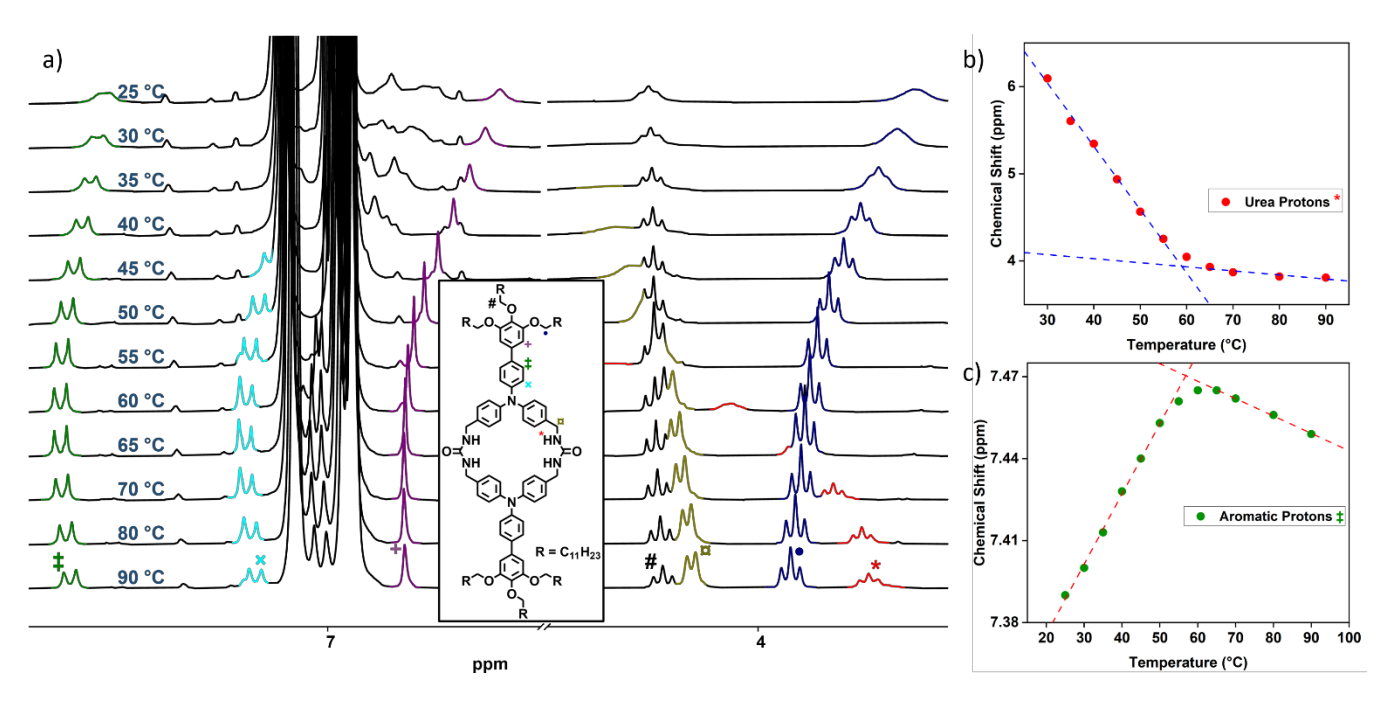


Figure 4 (a) Temperature-dependent ¹H NMR spectra for macrocycle **1**. Measurements were taken in toluene- d_8 at c = 1 mM and 400 MHz. The sample was methodically cooled from 90 °C to 25 °C, stabilizing for 5 min at every temperature. Inset: Structure of macrocycle **1**, highlighting the specific protons associated with the NMR peaks. Plot of chemical shift vs. temperature for (b) urea protons* and (c) aromatic protons‡ (7.38-7.47 ppm).

Earlier assembly reports in THF showed fiber formation but no gelation.²⁴ In comparison, toluene is less polar 2.4 versus 4.28 Both solvents can fit inside the macrocycle cavity as shown through crystal structures of model compound 2, which possesses a similar internal cavity. The single-crystal X-ray diffraction of 2 • toluene (Figure S8), establishes a host-to-guest ratio of 1:0.4, which is likely a lower estimate given toluene vapor pressure. Toluene as a small aromatic molecule may both fill interior cavities as well as have additional secondary interactions with TPAs that line the exterior 1, contributing to its gelation. To test if both interior templation and exterior aryl interactions are important, we examine solutions of 1 in mesitylene, which is too large to fit within the void of 1 (Figure S10). Our attempt to dissolve 1 in mesitylene followed a pattern like that of toluene, requiring heating to 60 °C for dissolution at a 1 mM concentration. However, prolonged equilibration at room temperature gave only precipitation and not gelation. The differing behavior of 1 in solvents like THF, toluene, and mesitylene highlights the significance of the solvent molecules occupying the internal cavity of the assembled structure, as well as the impact of external secondary interactions in the gelation process.

NMR Studies of Sol Phase. Next, the self-assembly of macrocycle **1** in the sol phase was studied using 1 H NMR spectroscopy in toluene- d_8 . At 25°C, the NMR spectra revealed broad peaks in both the aromatic and aliphatic regions (Figure S11), likely indicative of supramolecular polymerization. Notably, the absence of signals corresponding to methylene and urea protons can be attributed to significant broadening, a phenomenon commonly associated with self-assembly processes.

Temperature-dependent ¹H NMR measurements of macrocycle **1** were next used to probe the assembly behavior.

The sample (1 mM in toluene-*d*₈) was methodically cooled from 90 °C to 25 °C with a period of equilibration for 5 minutes at each temperature. At 90 °C, the ¹H NMR spectra exhibits well-defined peaks with distinct splitting patterns, likely indicative of monomeric form (Figure 4a, bottom spectra). However, as the temperature was lowered, the urea NHs show a downfield shift of approximately 1.75 ppm with substantial peak broadening. This downfield shift is indicative of intermolecular hydrogen bonding, while the broadening points to an increase in aggregation.²⁹

Except for the aromatic protons adjacent to the methylene ureas, which are obscured by the toluene signals, all other resonances display clear shifts with temperature. The variation in chemical shift as a function of temperature for the urea protons (Figure 4b), and aromatic protons (7.38-7.47 ppm, Figure 4c) suggests two types of assembly processes occur, with a change around 50-60 °C. For example, between 50-60 °C the aromatic protons (δ = 7.38-7.47‡, Figure 4c) transitioned from a downfield shift to a pronounced upfield shift. Other protons displayed a trend change, shifting significantly in the same direction (Figures 4b, S12b & S12c). This is indicative of an alteration in aggregation behavior in this temperature range and is consistent observations in the UV-vis studies at these temperatures.

2D DOSY NMR studies were used to examine the variations in particle sizes at different temperatures. These studies were executed under similar conditions to those of ^{1}H NMR, with the toluene- d_{θ} sample at a concentration of 1.3 mM and a frequency of 500 MHz. It was noted that the diffusion coefficient increased with temperature, showing a range from D = 1.6 x 10^{-10} m²s⁻¹ at 25 °C to D = 5.11 x 10^{-10} m²s⁻¹ at 80 °C (Figure S13). As it is customary for the diffusion coefficient to rise with temperature, the size of toluene- d_{θ} at a specific temperature was employed as a benchmark

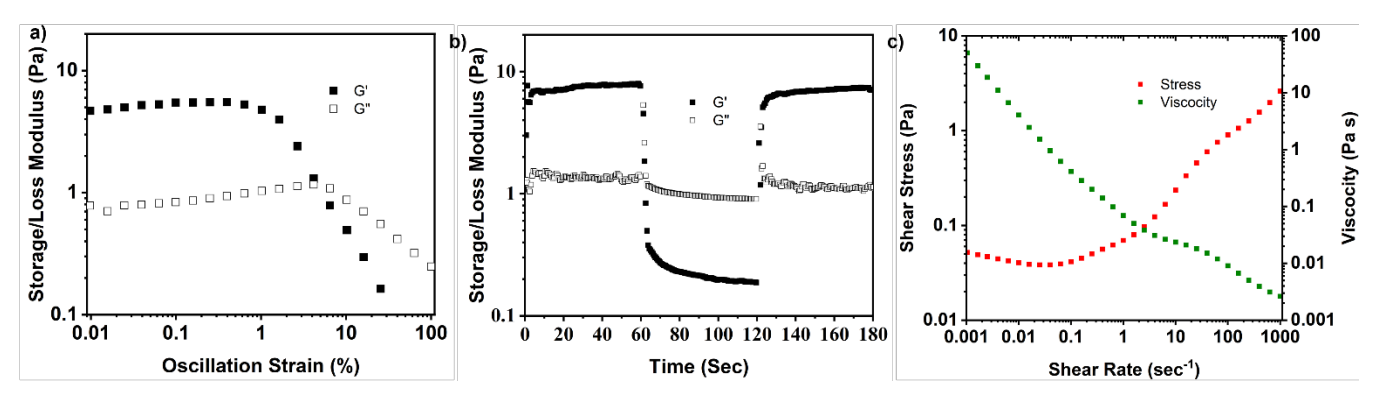


Figure 5. Rheological measurements taken for gel 1 at a concentration of 2 mM and at 10 °C. (a) Moduli vs oscillation strain obtained from an amplitude sweep test at a constant angular frequency (ω) of 10.0 rads⁻¹. (b) Thixotropic behavior of the gel shown by the moduli vs time plot obtained by subjecting the gel to various strain cycle. (c) Plot of stress and viscosity as a function of shear rate..

against the size of the assembly at corresponding temperatures.

The Stokes-Einstein equation was used for radius approximation. It is represented as:

$$D = \frac{k_B T}{6\pi \eta r}$$

Here, 'r' signifies the particle's radius, ' η ' represents the dynamic viscosity, 'T'' is the absolute temperature, and ' k_B ' is the Boltzmann constant. Based on this equation and assuming the radius of toluene (r_{tol}) is constant across all temperatures, the relative radius of the aggregate at 25 °C, 40 °C, 65 °C, and 80 °C are calculated as $8.5r_{tol}$, $6.72r_{tol}$, $5.92r_{tol}$, and $5.32r_{tol}$, respectively. This reveals a clear trend: as the temperature rises, the aggregate's radius diminishes. Specifically, it decreases from being 8.5 times the radius of toluene at 25 °C to just 5.32 times at 80 °C.

Rheological Study: Gelation under Mechanical Stim**uli.** The gelation behavior of **1** was probed by rheological experiments. Freshly prepared gel from 1 was examined at a fixed temperature of 10 °C. To achieve ideal gelation, a 2 mM concentration was utilized to ensure resilient rheological properties. Initially, we assessed the viscoelastic properties of the gel using an amplitude sweep test at a constant angular frequency (ω) of 10.0 rads⁻¹ (Figure 5a). The results indicated that gel 1 exhibited a linear viscoelastic region, where both the storage modulus (G') and the loss modulus (G") of the gel remained relatively constant up to a strain value of 0.6%. Beyond this point, G' began to decrease indicating the non-linear yielding of the gel-like structure. Notably, the substantial difference between G' and G" (G'>G") within the linear viscoelastic region confirmed the elastic nature of the sample. As the strain values increased, G' gradually decreased, and G" started to dominate. For strain values exceeding 4.56%, G">G', signifying the yielding behavior with the complete disruption of the gel network.

The self-healing properties of gel 1, as observed in our preliminary experiment in earlier section, prompted us to further investigate this thixotropic behavior using rheological analysis. To accomplish this, the gel underwent a series of controlled strain cycles at $10\,^{\circ}\text{C}$. Initially, it was subjected to a low strain of 0.1% within the linear viscoelastic region, for $60\,\text{s}$. This was followed by a higher strain of 50.0% for $60\,\text{s}$, intended to yield the gel network. Finally, the gel was allowed to recover by adjusting the strain back to 0.1% for

600 s, all at a constant angular frequency (ω) of 10.0 rads⁻¹. Upon subjecting the gel to a high strain of 50%, the G' value decreased significantly from 7.86 Pa to 0.19 Pa, while the G'' value exhibited a less pronounced decrease, reducing from 1.4 Pa to 0.9 Pa. This high strain level resulted in the complete yielding of the gel, rendering it more viscous than elastic, as evidenced by G''>G'. However, when the strain was reduced back to 0.1%, the G' value showed rapid recovery. Within the initial 3 s, it had already recovered by 67%, followed by an 88% recovery in the next 15 s, ultimately achieving complete recovery within the subsequent 30 s. Over time, both G' and G'' returned to their original values, with G'>G'', indicating the successful reformation of the gel.

In the rheological analysis, the viscosity of gel 1 was determined by measuring stress as a function of shear rate. We systematically applied shear rates ranging from 1000 s-1 down to 0.001 s⁻¹ at a temperature of 10 °C. Figure 5c illustrates the relationship between stress and viscosity in response to shear rate variations. It is noteworthy that stress exhibited an inverse proportionality to shear rate, while viscosity displayed a direct relationship with shear rate. This non-linear correlation between stress and shear rate is indicative of a non-Newtonian fluid behavior. Additionally, the decrease in viscosity with increasing shear rate classifies gel 1 as a shear-thinning liquid. Moreover, the shear stress plot indicates that the shear stress at low shear rates (below 0.1 s⁻¹) remains within the range of 0.04-0.05 Pa. The upward trend in shear stress, observed at shear rates above 0.1 s⁻¹, signifies the disruption of the gel-like network, indicative of an approximate yield stress of 0.05 Pa.

Rheological Study: Impact of Chain Stoppers on Gel 1. Based on our studies of the assembly process in the sol phase, it was evident that 1 primarily aggregates through intermolecular hydrogen bonding between the urea protons. The bifunctional urea groups play a crucial role in facilitating chain propagation during the assembly. Thus, addition of chain stoppers with competitive hydrogen bond acceptors should bind to chain ends and interrupt propagation, reducing the chain length. Notably, sulfoxide (β = 8.9), being a superior hydrogen acceptor compared to urea (β = 8.3), serves as an excellent candidate for a chain stopper.³⁰ Previous work found a decrease in the aggregate size of 1 in H₂O/THF solution upon the addition of diphenyl sulfoxide (DPS).²⁴ Therefore, dimethyl sulfoxide (DMSO) and DPS were investigated as chain stoppers and their effects on the gel storage and loss modulus were tested.

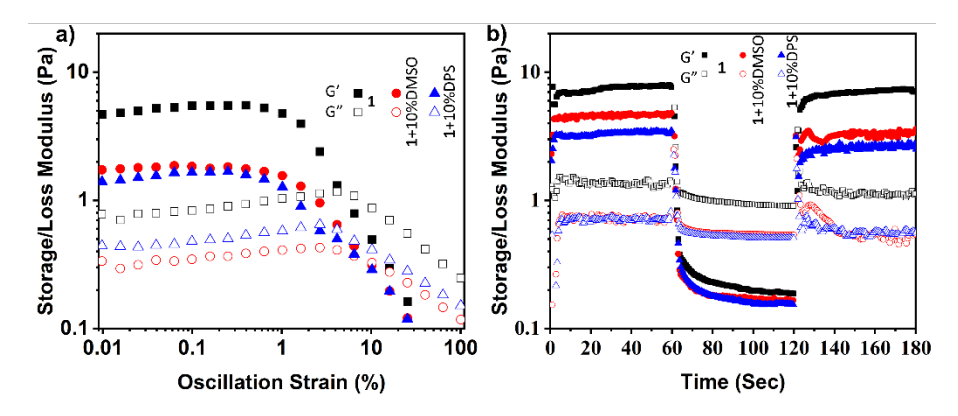


Figure 6 Rheological studies with **1**+10% chain stoppers (DMSO and DPS) at concentration of 2 mM and 10 °C. (a) Moduli vs oscillation strain obtained from an amplitude sweep test at a constant angular frequency (ω) of 10.0 rads⁻¹. (b) Thixotropic behavior of the gel shown by the moduli vs time plot obtained by subjecting the gel to various strain cycle

Like prior measurements, gel samples were prepared by maintaining a constant concentration of ${\bf 1}$ at 2 mM in toluene, with 10% chain stoppers. The viscoelastic properties of these samples were then assessed using an amplitude sweep test, following the same procedures as before. Thixotropic behavior was subsequently explored by subjecting the gels to a series of controlled strain cycles. These cycles were all conducted at a fixed angular frequency (ω) of 10.0 rads⁻¹ and maintained at a consistent temperature of 10 °C (Figure 6).

Figure 6a shows the amplitude sweep test, which revealed linear viscoelastic regions for all three samples. At strains below 1%, the storage modulus (G') for $\bf 1$ was significantly higher than that of $\bf 1+10\%$ DMSO and $\bf 1+10\%$ DPS, before all samples eventually collapsed. This indicates that $\bf 1$ forms a more robust gel compared to those containing chain stoppers. At the lower strain values, the difference between the storage modulus (G') and the loss modulus (G'') for $\bf 1$, $\bf 1+10\%$ DMSO, and $\bf 1+10\%$ DPS was around 4.2 Pa, 1.5 Pa, and 1 Pa, respectively, with $\bf 1$ exhibiting the greatest values, thus underscoring its superior gelation behavior. For all examined strain values, G'' for the samples with chain stoppers was consistently lower than for $\bf 1$.

Figure 6b compares the thixotropic properties of the three samples. At the lower strain of 0.1%, all samples showed G' greater than G", indicative of gel formation. Within this regime, the G' values ranked from highest to lowest as follows: 1 >1+10% DMSO >1+10% DPS, indicating that 1 forms the most robust gel, while the gel with 1+10% DPS was the weakest. When the strain was increased to 50%, gels in all samples were disrupted, with similar G' values observed across the board. On reverting the strain back to 0.1%, gel reformation was evident. G' for 1 almost completely recovered within 30 s, reaching 97% of its initial value, while 1+10% DMSO and 1+10% DPS showed lower recoveries at 67% and 76%, respectively. The slower and incomplete recovery of the samples containing chain stoppers, in contrast to pure **1**, is attributable to the impact of these chain stoppers on the intermolecular hydrogen bonding and kinetics of the self-assembly. In summary, the presence of chain stoppers not only reduced the strength of the gels but also led to a more protracted recovery phase.

CONCLUSION

In conclusion, this study explores the gelation behavior of dendronized triphenylamine bis-urea macrocycle **1** in toluene. Notably, **1** exhibited remarkable gel formation at an impressively low critical gelation concentration (CGC) of 0.066 wt%, categorizing it as a super-gelator. Micrographs of the dried gels highlighted their fibrillar networks. Furthermore, **1** displayed a thermoreversible gel-sol phase transition in toluene, demonstrating the ability to switch between gel and sol phases when heated to 60 °C and subsequently cooled to room temperature. The self-healing behavior of **1** was also observed, emphasizing its robust gel properties.

Assembly processes in the sol state were investigated using UV-Vis and NMR spectroscopy to provide further evidence of the assembly transition between 50-60 °C. Temperature-dependent 1H NMR studies in toluene- d_8 , show the urea protons shift downfield and become broader as the temperature decreases, consistent with intermolecular hydrogen bonding. Interestingly, plots of the change in molecular shifts of other resonances, show consistent changes between 90 to ~ 60 °C, suggesting hydrogen bonding and π - π stacking of the monomers. Moreover, a transition observed between 50-60°C likely indicates the formation of a network. The 2D DOSY NMR revealed an inverse relationship between aggregate size and temperature in the sol phase, further supporting the assembly dynamics of compound 1.

Rheological experiments provided deeper insight into the gel behavior of 1 at 10 °C. The amplitude sweep test unveiled a linear viscoelastic region at strain values below 0.6%, with a marked disparity between G' and G", affirming the formation of a gel-like material. A series of strain cycles highlighted the thixotropic behavior of gel 1 and its rapid recovery within 30 s. Intriguingly, sulfoxides, DMSO and DPS with their competitive hydrogen bond acceptors (β = 8.9 versus urea $\beta = 8.3$) exhibited a marked impact on the gelation properties with chain stoppers leading to a weaker gel formation. In addition, the 1+10% chain stopper samples displayed only partial recovery relative to the pure 1 gel, underscoring the notable impact of chain stoppers on both gel strength and recovery properties. Our next goal is to probe the accessibility of these gels to guests and additives and investigate their application as confined environments for reaction.

ASSOCIATED CONTENT

Supporting Information. Synthetic procedures, NMR, UV-vis, and Rheology data. CCDC Deposition number 2308796

contains the supplementary crystallographic data. This material is available free of charge via the Internet at http://pubs.acs.org.

AUTHOR INFORMATION

Corresponding Author

* Linda S. Shimizu – Department of Chemistry and Biochemistry, University of South Carolina, Columbia, South Carolina, 29208, United State; orcid.org/0000-0001-5599-4960; Email: shimizuls@mailbox.sc.edu.

Author Contributions

L.S.S. initiated the study. R.P., M. E., F. G., M. S. and L.S.S. planned experiments, analyzed data and contributed to the manuscript. R.P., M. E., and F. G. performed experiments. The manuscript was written through contributions of all authors. All authors have given approval to the final version of the manuscript.

Funding Sources

This work was supported in part by the National Science Foundation (NSF) CHE-2203830 and OIA-1655740. M. S. was supported by the NSF under award 2146428. Any opinions, findings and conclusions, and recommendations expressed in this material are those of the authors and do not necessarily reflect those of the NSF.

ACKNOWLEDGMENT

We thank Dr. Perry J. Pellechia for assistance with DOSY NMR experiments and helpful discussions.

ABBREVIATIONS

DMSO, dimethyl sulfoxide; DPS, diphenyl sulfoxide; CGC, critical gelation concentration; THF, tetrahydrofuran; TPA, triphenylamine; .

REFERENCES

- (1) de Jong, J. J. D.; Feringa, B. L.; van Esch, J. Responsive Molecular Gels. In Molecular Gels: Materials with Self-Assembled Fibrillar Networks; Weiss, R. G., Terech, P., Eds.; Springer Netherlands: Dordrecht, 2006; pp 895–927. https://doi.org/10.1007/1-4020-3689-2_27.
- (2) Molecules | Free Full-Text | Smart and Functional Conducting Polymers: Application to Electrorheological Fluids. https://www.mdpi.com/1420-3049/23/11/2854 (accessed 2023-10-18).
- (3) Liu, K.; Zang, S.; Xue, R.; Yang, J.; Wang, L.; Huang, J.; Yan, Y. Coordination-Triggered Hierarchical Folate/Zinc Supramolecular Hydrogels Leading to Printable Biomaterials. *ACS Appl. Mater. Interfaces* **2018**, *10* (5), 4530–4539. https://doi.org/10.1021/acsami.7b18155.
- (4) Mredha, Md. T. I.; Guo, Y. Z.; Nonoyama, T.; Nakajima, T.; Kurokawa, T.; Gong, J. P. A Facile Method to Fabricate Anisotropic Hydrogels with Perfectly Aligned Hierarchical Fibrous Structures. *Adv. Mater.* 2018, *30* (9), 1704937. https://doi.org/10.1002/adma.201704937.
- (5) Shi, Y.; Ma, C.; Peng, L.; Yu, G. Conductive "Smart" Hybrid Hydrogels with PNIPAM and Nanostructured Conductive Polymers. Adv. Funct. Mater. 2015, 25 (8), 1219–1225. https://doi.org/10.1002/adfm.201404247.
- (6) Ma, Z.; Zhang, P.; Yu, X.; Lan, H.; Li, Y.; Xie, D.; Li, J.; Yi, T. Sugar Based Nanotube Assembly for the Construction of Sonication Triggered Hydrogel: An Application of the Entrapment of Tetracycline Hydrochloride. J. Mater. Chem. B 2015, 3 (37), 7366–7371. https://doi.org/10.1039/C5TB01191D.
- (7) Buerkle, L. E.; Rowan, S. J. Supramolecular Gels Formed from Multi-Component Low Molecular Weight Species.

- *Chem. Soc. Rev.* **2012**, 41 (18), 6089–6102. https://doi.org/10.1039/C2CS35106D.
- (8) Fang, W.; Zhang, Y.; Wu, J.; Liu, C.; Zhu, H.; Tu, T. Recent Advances in Supramolecular Gels and Catalysis. *Chem. Asian J.* 2018, 13 (7), 712–729. https://doi.org/10.1002/asia.201800017.
- (9) Banerjee, S.; Das, R. K.; Maitra, U. Supramolecular Gels 'in Action.' J. Mater. Chem. 2009, 19 (37), 6649–6687. https://doi.org/10.1039/B819218A.
- (10) Steed, J. W. Supramolecular Gel Chemistry: Developments over the Last Decade. *Chem. Commun.* **2011**, *47* (5), 1379–1383. https://doi.org/10.1039/C0CC03293I.
- (11) Yu, G.; Yan, X.; Han, C.; Huang, F. Characterization of Supramolecular Gels. *Chem. Soc. Rev.* 2013, 42 (16), 6697–6722. https://doi.org/10.1039/C3CS60080G.
- (12) He, X.; Fan, J.; Wooley, K. L. Stimuli-Triggered Sol–Gel Transitions of Polypeptides Derived from α-Amino Acid N-Carboxyanhydride (NCA) Polymerizations. *Chem. Asian J.* **2016**, 11 (4), 437–447. https://doi.org/10.1002/asia.201500957.
- (13) Zacharias, S. C.; Kamlar, M.; Sundén, H. Exploring Supramolecular Gels in Flow-Type Chemistry—Design and Preparation of Stationary Phases. *Ind. Eng. Chem. Res.* 2021, 60 (28), 10056–10063. https://doi.org/10.1021/acs.iecr.1c01914.
- (14) Foster, J. A.; Steed, J. W. Exploiting Cavities in Supramolecular Gels. *Angew. Chem. Int. Ed.* 2010, 49 (38), 6718–6724. https://doi.org/10.1002/anie.201000070.
- (15) Yan, X.; Wang, F.; Zheng, B.; Huang, F. Stimuli-Responsive Supramolecular Polymeric Materials. *Chem. Soc. Rev.* 2012, 41 (18), 6042–6065. https://doi.org/10.1039/C2CS35091B.
- (16) Chang, J.; Zhao, Q.; Kang, L.; Li, H.; Xie, M.; Liao, X. Multire-sponsive Supramolecular Gel Based on Pillararene-Containing Polymers. *Macromolecules* 2016, 49 (7), 2814–2820. https://doi.org/10.1021/acs.macromol.6b00270.
- (17) Li, Y.-F.; Li, Z.; Lin, Q.; Yang, Y.-W. Functional Supramolecular Gels Based on Pillar[n]Arene Macrocycles. *Nanoscale* **2020**, 12 (4), 2180–2200. https://doi.org/10.1039/C9NR09532B.
- (18) Ide, T.; Takeuchi, D.; Osakada, K. Columnar Self-Assembly of Rhomboid Macrocyclic Molecules via Step-like Intermolecular Interaction. Crystal Formation and Gelation. *Chem. Commun.* 2011, 48 (2), 278–280. https://doi.org/10.1039/C1CC15311K.
- (19) Xiao, T.; Xu, L.; Zhou, L.; Sun, X.-Q.; Lin, C.; Wang, L. Dynamic Hydrogels Mediated by Macrocyclic Host–Guest Interactions. J. Mater. Chem. B 2019, 7 (10), 1526–1540. https://doi.org/10.1039/C8TB02339E.
- (20) Qi, Z.; Schalley, C. A. Exploring Macrocycles in Functional Supramolecular Gels: From Stimuli Responsiveness to Systems Chemistry. Acc. Chem. Res. 2014, 47 (7), 2222–2233. https://doi.org/10.1021/ar500193z.
- (21) Sindt, A. J.; DeHaven, B. A.; Goodlett, D. W.; Hartel, J. O.; Ayare, P. J.; Du, Y.; Smith, M. D.; Mehta, A. K.; Brugh, A. M.; Forbes, M. D. E.; Bowers, C. R.; Vannucci, A. K.; Shimizu, L. S. Guest Inclusion Modulates Concentration and Persistence of Photogenerated Radicals in Assembled Triphenylamine Macrocycles. J. Am. Chem. Soc. 2020, 142 (1), 502–511. https://doi.org/10.1021/jacs.9b11518.
- [22] Islam, M. F.; Adame-Ramirez, E.; Williams, E. R.; Kittikhunnatham, P.; Wijesekera, A.; Zhang, S.; Ge, T.; Stefik, M.; Smith, M. D.; Pellechia, P. J.; Greytak, A. B.; Shimizu, L. S. Inclusion Polymerization of Pyrrole and Ethylenedioxythiophene in Assembled Triphenylamine Bis-Urea Macrocycles. *Macromolecules* 2022, 55 (24), 11013–11022. https://doi.org/10.1021/acs.macromol.2c02042.
- (23) Goodlett, D. W.; Sindt, A. J.; Islam, M. F.; Smith, M. D.; Shimizu, L. S. Selective Loading of Xylene Isomers in Self-Assembled Triphenylamine Bis-Urea Macrocycles. *Cryst. Growth Des.* 2022, 22 (2), 1017–1023. https://doi.org/10.1021/acs.cgd.1c00846.

- (24) Prakash, R.; Islam, M. F.; Kothalawala, R. M.; Hossain, M. S.; Smith, M. D.; Shimizu, L. S. Cooperative Supramolecular Polymerization of Triphenylamine Bis-Urea Macrocycles. *Chem. – Eur. J.* 2023, 29 (36), e202300698. https://doi.org/10.1002/chem.202300698.
- (25) Dong, S.; Zheng, B.; Xu, D.; Yan, X.; Zhang, M.; Huang, F. A Crown Ether Appended Super Gelator with Multiple Stimulus Responsiveness. *Adv. Mater.* 2012, 24 (24), 3191–3195. https://doi.org/10.1002/adma.201200837.
- (26) Núñez-Villanueva, D.; A. Jinks, M.; Magenti, J. G.; A. Hunter, C. Ultrasound-Induced Gelation of a Giant Macrocycle. *Chem. Commun.* 2018, 54 (77), 10874–10877. https://doi.org/10.1039/C8CC04742A.
- (27) Shin, G.; Khazi, M. I.; Kim, J.-M. Protonation-Triggered Supramolecular Gel from Macrocyclic Diacetylene: Gelation Behavior, Topochemical Polymerization, and Colorimetric Response. Langmuir 2020, 36 (46), 13971–13980. https://doi.org/10.1021/acs.langmuir.0c02469.
- (28) Snyder, L. R. Classification off the Solvent Properties of Common Liquids. *J. Chromatogr. Sci.* **1978**, *16* (6), 223–234. https://doi.org/10.1093/chromsci/16.6.223.
- (29) Matern, J.; Fernández, Z.; Bäumer, N.; Fernández, G. Expanding the Scope of Metastable Species in Hydrogen Bonding-Directed Supramolecular Polymerization. Angew. Chem. Int. Ed. 2022, 61 (26), e202203783. https://doi.org/10.1002/anie.202203783.
- (30) Hunter, C. A. Quantifying Intermolecular Interactions: Guidelines for the Molecular Recognition Toolbox. *Angew. Chem. Int. Ed.* **2004**, 43 (40), 5310–5324. https://doi.org/10.1002/anie.200301739.

